AD NUMBER

AD804001

LIMITATION CHANGES

TO:

Approved for public release; distribution is unlimited.

FROM:

Distribution authorized to U.S. Gov't. agencies and their contractors; Critical Technology; DEC 1966. Other requests shall be referred to Arnold Engineering Development Center, Armold AFS, TN. This document contains export-controlled technical data.

AUTHORITY

AEDC ltr, 17 Nov 1972

AEDC-TR-66-179

HEMISPHERE-CYLINDER PRESSURE DISTRIBUTIONS AT SUPERSONIC AND HYPERSONIC MACH NUMBERS

E. L. Clark

ARO, Inc.

December 1966

This document is subject to special export controls and each transmittal to foreign governments or foreign nationals may be made only with prior approval of Arnold Engineering Development Center (AETS), Arnold Air Force Station, Tennessee.

VON KÁRMÁN GAS DYNAMICS FACILITY
ARNOLD ENGINEERING DEVELOPMENT CENTER
AIR FORCE SYSTEMS COMMAND
ARNOLD AIR FORCE STATION, TENNESSEE

Approved for public release; distribution unlimited.

NOTICES

When U. S. Government drawings specifications, or other data are used for any purpose other than a definitely related Government procurement operation, the Government thereby incurs no responsibility nor any obligation whatsoever, and the fact that the Government may have formulated, furnished, or in any way supplied the said drawings, specifications, or other data, is not to be regarded by implication or otherwise, or in any manner licensing the holder or any other person or corporation, or conveying any rights or permission to manufacture, use, or sell any patented invention that may in any way be related thereto.

Qualified users may obtain copies of this report from the Defense Documentation Center.

References to named commercial products in this report are not to be considered in any sense as an endorsement of the product by the United States Air Force or the Government.

HEMISPHERE-CYLINDER PRESSURE DISTRIBUTIONS AT SUPERSONIC AND HYPERSONIC MACH NUMBERS

E. L. Clark
ARO, Inc.

AF - AEDC
Arnold AFS Tenn

FOREWORD

The work reported herein was done at the request of Headquarters, Arnold Engineering Development Center (AEDC), Air Force Systems Command (AFSC), under Program Element 65402234.

The results of research presented were obtained by ARO, Inc. (a subsidiary of Sverdrup & Parcel and Associates, Inc.), contract operator of AEDC, AFSC, Arnold Air Force Station, Tennessee, under Contract AF40(600)-1200. The research was conducted under ARO Project No. VT3116, and the manuscript was submitted for publication on August 25, 1966.

The author would like to express his appreciation to A. D. Ray of the Hypersonic Branch, von Kármán Gas Dynamics Facility (VKF), for his assistance in the experimental program, to C. H. Lewis of the Hypervelocity Branch, VKF, for providing the numerical solutions for spherically blunted cones, and to R. K. Matthews and L. L. Trimmer of the Hypersonic Branch, VKF, for furnishing unpublished experimental data at Mach numbers of 6, 8, and 10.

This technical report has been reviewed and is approved.

James N. McCready
Major, USAF
AF Representative, VKF
Directorate of Test

Leonard T. Glaser
Colonel, USAF
Director of Test

ABSTRACT

Pressure distributions on a hemisphere-cylinder at a Mach number of 10 and at angles of attack up to 25 deg are presented. These experimental distributions are compared with hypersonic blunt-body analytical and numerical solutions. Experimental stagnation point velocity gradients, sonic point locations, and pressure drag coefficients for hemispheres at Mach numbers from 1.8 to 21 have been compiled, and empirical relations are developed for these parameters as functions of Mach number.

CONTENTS

ILLUSTRATIONS

TABLES

NOMENCLATURE

a	Speed of sound
b_n	Coefficients in series for surface pressure
C_D	Pressure drag coefficient, $D/q_\infty \pi R^2$
C_p	Pressure coefficient, $(p - p_\infty)/q_\infty$
$C_{p_{max}}$	Stagnation point pressure coefficient, $(p_{t_2} - p_\infty)/q_\infty$
D	Drag or model diameter
M	Mach number
p	Static pressure
p_t	Total pressure
q	Dynamic pressure
R	Hemisphere radius of curvature
R_{e_D}	Free-stream Reynolds number based on model diameter
r	Local hemisphere radius normal to axis of symmetry
S	Surface distance measured from physical stagnation point ($\theta = 0$)
u	Velocity

α	Angle of attack
β	Stagnation point velocity gradient, du/dS
γ	Ratio of specific heats
δ	Cone half-angle
θ	Hemisphere surface angle measured from the physical stagnation point, i.e., the point where the surface tangent is normal to the free-stream flow
θ_m	Hemispherical model surface angle measured from axis of symmetry

SUBSCRIPTS

2	Conditions just downstream of a normal shock wave
B	Dimension associated with base of spherical segment
o	Conditions at $\theta = 0$
t	Total conditions
∞	Free-stream conditions

SUPERSCRIPTS

*	Conditions where the local speed is equal to the local speed of sound

SECTION I
INTRODUCTION

The development of ballistic missiles which re-enter the earth's atmosphere at hypersonic speeds has made the problem of aerodynamic heating one of primary importance. The heating is most severe at the nose, and since state-of-the-art cooling techniques preclude the use of a sharp nose, blunt-nosed vehicles are used. Therefore, the supersonic and hypersonic aerodynamic characteristics of blunt bodies have received considerable attention.

Theoretical studies of blunt-body flows followed many approaches as outlined by Van Dyke in Ref. 1. Two of the most successful appear to be the numerical method of Van Dyke (Refs. 1 and 2) and the empirical modifications of the Newtonian theory suggested by Lees and Kubota (Refs. 3 and 4). Concurrent with the theoretical studies, many experimental investigations, primarily at Mach numbers less than five, have been conducted (e.g., Refs. 5 through 20). The hemisphere, because of its simple geometry, has been the most extensively investigated of the various blunt bodies. Interest in the aerodynamic characteristics of the hemisphere, together with the knowledge that the pressure distribution on a hemisphere could be very sensitive to flow deviations in a wind tunnel, led to the adoption of this body as an AGARD calibration model (E) by the AGARD Wind Tunnel and Model Testing Panel in 1957 (Ref. 21).

The hemisphere-cylinder is a configuration which has been of practical concern since the early development stages of re-entry vehicles. There have been many theoretical and experimental studies of the hemisphere-cylinder at zero angle of attack, and Ref. 22 presents a summary of several of these studies. However, there have been very few investigations of the flow over a hemisphere-cylinder at angles of attack other than zero.

The purpose of the present investigation was to complement the results of the earlier experimental studies on hemispheres and hemisphere-cylinders by testing these bodies at a higher Mach number and, in the case of the hemisphere-cylinder, at angles of attack other than zero. By combining the present data with data from Refs. 5 through 20, a compilation of experimental results for hemispheres over a large range of Mach numbers could be made. Such a compilation would be of value in missile development studies and in wind tunnel calibrations.

The experimental tests described in this report were conducted in the 50-in. hypersonic tunnel (Gas Dynamic Wind Tunnel, Hypersonic (C)) of VKF, AEDC. Two models having diameters of 1.38 and 5.80 in. were tested at a nominal Mach number of 10 and at Reynolds numbers,

based on body diameter, of 0.15×10^6 and 0.63×10^6, respectively. The angle-of-attack range was from 0 to 25 deg.

SECTION II
APPARATUS AND PRECISION OF MEASUREMENTS

2.1 TEST FACILITY

Tunnel C is an axisymmetric, continuous flow, variable-density wind tunnel with a 50-in.-diam test section. The contoured nozzle produces a nominal test section Mach number of 10 at stagnation pressures from 200 to 2000 psia and stagnation temperatures up to 1900°R. Further details on Tunnel C are given in Ref. 23.

The present tests were conducted at a Mach number of 10.05 with a stagnation pressure of 1000 psia and a stagnation temperature of 1850°R, producing a free-stream unit Reynolds number of 0.108×10^6 per inch.

2.2 MODELS

Two hemisphere-cylinder models were utilized in the test program. A large model having a diameter of 5.80 in. and a length of 38 in. was used to obtain the hemisphere data. The cylindrical portion of this model was used to obtain cylinder data for length-to-diameter ratios of 0.5 to 6. Pressure orifices were located around the hemisphere in 10-deg increments and along the cylinder in approximately 2-in. intervals. The orifices were 0.067 in. in diameter and were located within a tolerance of ±0.2 deg on the hemisphere. A small model having a diameter of 1.38 in. and a length of 39 in. was used to obtain cylinder data for length-to-diameter ratios of 1 to 28. With the exception of an orifice at the geometrical stagnation point, this model had no orifices on the hemisphere.

2.3 PRECISION OF MEASUREMENTS

Several sources of error were present in the experiment. These errors may be considered as being in two categories - fixed and random. The fixed errors which were present throughout the test included transducer nonlinearities and free-stream Mach number uncertainties. The random errors varied during the tests and included instrument zero shifts, angle-of-attack inaccuracies, dimensional inaccuracies in orifice locations (considered as random in this test because the data were analyzed

using $|\theta_m + \alpha|$ as the surface angle, thus incorporating several combinations of orifice location and angle of attack into each averaged value), and model distortions attributable to thermal gradients from the windward to leeward side. The absolute errors could be evaluated from transducer and tunnel calibrations, and the random errors were estimated by comparing a number of repeat runs with the two models. The indicated total uncertainties in the data are given in the table below:

p/p_{t_2}	1.0 to 0.2	0.2 to 0.04	0.04 to 0.008
Uncertainty, percent	±1 to 3	±3 to 5	±5 to 10

SECTION III
RESULTS AND DISCUSSION

3.1 HEMISPHERE

The experimental surface pressure distribution over the hemisphere at Mach number 10.05 is presented in Fig. 1a. In this figure, the surface pressure has been normalized with respect to the stagnation pressure behind a normal shock, p_{t_2}. The abscissa of the plot, $\theta = |\theta_m + \alpha|$, is the absolute value of the angle between an orifice and the physical stagnation point, i.e., the point where the surface tangent is normal to the free-stream flow. As was mentioned previously, the orifices were spaced in 10-deg increments from $\theta_m = -90$ to 90 deg, and the angle of attack was varied from 0 to 25 deg in 5-deg increments. Combinations of θ_m and α allowed four to six pressure measurements to be made at each value of θ. Since there was no measurable effect of the cylindrical afterbody on the hemisphere pressures, the data points shown in Fig. 1a are arithmetical averages of the measurements, and the repeatability of the data was within the uncertainty limits presented in Section 2.3. These averaged pressure ratios are also tabulated in Table I.

A comparison of the experimental results with two blunt-body theories is presented in Fig. 1b. The theoretical distribution determined by matching a method of characteristics solution to the Van Dyke numerical solution at a surface Mach number of 1.05 ($\theta = 42.8$ deg) was obtained from calculations by C. H. Lewis of VKF. The calculation procedure is described in Ref. 24. This distribution is in excellent agreement with the experimental results for $\theta = 0$ to 50 deg. At angles greater than 50 deg, the experimental data are above the theoretical curve. This discrepancy may be the result of boundary-layer growth on the hemisphere which effectively increases the local surface inclination and, hence, the surface pressure. The influence of viscous effects on the pressure at the shoulder ($\theta = 90$ deg) is discussed later. The distribution

predicted by the modified Newtonian theory (Ref. 3) is higher than the experimental data for θ = 0 to 60 deg. For angles greater than 60 deg, the theory predicts a too rapidly decreasing pressure and is substantially in error at θ = 90 deg. Matching the modified Newtonian theory to a Prandtl-Meyer expansion (Ref. 4) at θ = 55.2 deg (M = 1.36), which is the point on the surface where both the pressure and pressure gradient predicted by these two solutions are equal, greatly improves the theoretical estimate for $\theta > 60$ deg.

Three aerodynamic characteristics of a hemisphere which may be determined from the pressure distribution are the stagnation point velocity gradient, the sonic point location, and the pressure drag coefficient. These characteristics have been determined from the experimental pressure distribution and are discussed in the following paragraphs.

The stagnation point velocity gradient is of considerable importance since it has been shown, by Fay and Riddell (Ref. 25) and others, that the stagnation point heat transfer is proportional to the square root of this parameter. The stagnation point velocity gradient may be presented in several forms. The Mach number gradient, $(dM/d\theta)_o$, is used in this report because it is relatively insensitive to the free-stream Mach number and, as will be shown later, when the velocity gradient is in this form, it may be correlated as a function of $1/M_\infty^2$. Other forms of the velocity gradient may be easily obtained from the Mach number gradient, for example:

$$\left(\frac{du}{dS}\right)_o = \frac{a_t}{R}\left(\frac{dM}{d\theta}\right)_o \text{, 1/sec} \tag{1}$$

$$\frac{\beta D}{u_\infty} \equiv \left(\frac{du}{dS}\right)_o \frac{D}{u_\infty} = \frac{\sqrt{2(\gamma+1)}}{u_\infty/a^*}\left(\frac{dM}{d\theta}\right)_o = 2\left[\frac{2+(\gamma-1)M_\infty^2}{2M_\infty^2}\right]^{1/2}\left(\frac{dM}{d\theta}\right)_o \tag{2}$$

$$\frac{\beta D}{u_2} \equiv \left(\frac{du}{dS}\right)_o \frac{D}{u_2} = \sqrt{2(\gamma+1)}\left(\frac{u_\infty}{a^*}\right)\left(\frac{dM}{d\theta}\right)_o = (\gamma+1)\left[\frac{2M_\infty^2}{2+(\gamma-1)M_\infty^2}\right]^{1/2}\left(\frac{dM}{d\theta}\right)_o \tag{3}$$

To determine the surface Mach number, it is assumed that the flow over the hemisphere, at the outer edge of the boundary layer, is isentropic with a stagnation pressure equal to p_{t_2}. The correctness of this assumption has been verified experimentally (e.g., Ref. 9). The local Mach number may then be obtained from the isentropic relation,

$$\frac{p}{p_{t_2}} = \left(1 + \frac{\gamma-1}{2}M^2\right)^{-\frac{\gamma}{\gamma-1}} \tag{4}$$

Differentiating Eq. (4) with respect to θ and rearranging terms gives

$$\frac{dM}{d\theta} = - \frac{\left(1 + \frac{\gamma-1}{2} M^2\right)^{\frac{2\gamma-1}{\gamma-1}}}{\gamma M} \frac{d\left(p/p_{t_2}\right)}{d\theta} \tag{5}$$

Since both $d(p/p_{t_2})/d\theta$ and M are equal to zero at $\theta = 0$, an alternate form is necessary. From the modified Newtonian theory,

$$\left(\frac{P}{P_{t_2}}\right)_{Newtonian} = 1 - \left(1 - \frac{P_\infty}{P_{t_2}}\right) \sin^2\theta \tag{6}$$

and

$$\left[\frac{d\left(p/p_{t_2}\right)}{d \sin^2\theta}\right]_{Newtonian} = - \left(1 - \frac{P_\infty}{P_{t_2}}\right) \tag{7}$$

Since the Newtonian theory shows that the derivative of p/p_{t_2} with respect to $\sin^2\theta$ is constant for a given Mach number, it can be assumed that the derivative, at least for small values of θ, will be nearly constant for experimental data. The experimental distribution is plotted as a function of $\sin^2\theta$ in Fig. 2a, and it is seen that the slope of the curve is essentially constant for values of θ less than 20 deg. Thus, an accurate value of $d(p/p_{t_2})/d(\sin^2\theta)$ may be obtained from the experimental data. Equation (5) is then rewritten as

$$\frac{dM}{d\theta} = - \frac{\sin 2\theta \left(1 + \frac{\gamma-1}{2} M^2\right)^{\frac{2\gamma-1}{\gamma-1}}}{\gamma M} \frac{d\left(p/p_{t_2}\right)}{d(\sin^2\theta)} \tag{8}$$

Evaluating this relation at $\theta = 0$ gives

$$\left(\frac{dM}{d\theta}\right)_o = \sqrt{- \left(\frac{2}{\gamma}\right) \frac{d\left(p/p_{t_2}\right)}{d(\sin^2\theta)}} \tag{9}$$

From Fig. 2a and Eq. (9) it is determined that $(dM/d\theta)_o = 1.27$ for the $M_\infty = 10.05$ experimental data. The modified Newtonian and Van Dyke theoretical solutions are also shown in Fig. 2a and give values of 1.19 and 1.30, respectively for $(dM/d\theta)_o$ at $M_\infty = 10$.

The sonic point location, θ^*, is the point on the hemisphere where the local Mach number, at the outer edge of the boundary layer, is equal to unity. Since isentropic flow has been assumed, the sonic point location is that value of θ at which $p/p_{t_2} = 0.528$. For the present data, $\theta^* = 41.5$ deg. Modified Newtonian and Van Dyke theoretical solutions give sonic point locations of 43.5 and 40.6 deg, respectively, at $M_\infty = 10$.

The current trend in re-entry vehicles is toward slender, low drag configurations. For this type of body the drag of a spherical nose may be

70 to 80 percent of the vehicle's total pressure drag. Therefore, it is essential to have accurate experimental measurements of the drag of spherical segments. The forebody pressure drag on a spherical segment is given by

$$D = 2\pi \int_0^{r_B} (p - p_\infty)\, r\, dr \tag{10}$$

where r is the local radius and r_B is the base radius as shown below.

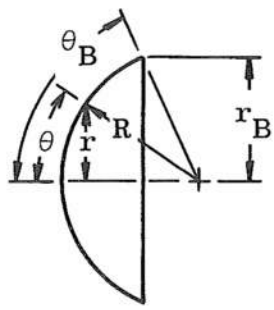

In coefficient form, referenced to the area, πR^2,

$$C_D = \frac{2}{\gamma M_\infty^2} \int_0^{(r_B/R)^2} \left(\frac{p}{p_\infty} - 1\right) d\left(\frac{r}{R}\right)^2$$

or in terms of θ,

$$C_D = \frac{2}{\gamma M_\infty^2} \int_0^{\sin^2\theta_B} \left(\frac{p}{p_\infty} - 1\right) d(\sin^2\theta)$$

then,

$$C_D = \frac{2}{\gamma M_\infty^2} \left[\left(\frac{p_{t_2}}{p_\infty}\right) \int_0^{\sin^2\theta_B} \left(\frac{p}{p_{t_2}}\right) d(\sin^2\theta) - \sin^2\theta_B\right] \tag{11}$$

Thus, C_D can be determined by graphical or numerical integration from a plot of p/p_{t_2} versus $\sin^2\theta$ (Fig. 2b). The results of an integration of the experimental data are shown in Fig. 3 where C_D is plotted as a function of the base angle, θ_B. For spherical segments with $\theta_B < \theta^*$ the drag coefficient is only approximate since cutting a sphere ahead of the characteristic sonic point will force the sonic point to be located on the shoulder. This will modify the pressure distribution and, consequently, the drag. Unpublished experimental results (Trimmer, VKF) obtained at $M_\infty = 10$ on two models with $\theta_B = 14.3$ and 30.0 deg are presented in Fig. 3 as an indication of the drag reduction which results from cutting a sphere ahead of the sonic point. The experimental drag coefficient of the full hemisphere ($\theta_B = 90$ deg) is 0.90. The drag coefficients calculated from the modified

Newtonian and Van Dyke-method of characteristics theoretical solutions are included in Fig. 3 and for the full hemisphere have values of 0.92 and 0.87, respectively.

A correlation of the data obtained in the present tests with previously published results (Refs. 5 through 20) is presented in Figs. 4 through 7. The references used in these correlations were restricted to those containing data obtained at Mach numbers greater than 1.8 with models having a diameter of 1.0 in. or larger. Included in these figures are unpublished data obtained at Mach numbers of 6, 8, and 10 by R. K. Matthews and L. L. Trimmer of VKF, using the 5.80-in.-diam model described in Section 2.2. A tabulation of model sizes and test conditions for the referenced data is given in Table II.

The experimental surface pressure distribution on a hemisphere at Mach numbers from 1.9 through 21 are shown in Fig. 4. Twelve sources of data were used in obtaining the data fairings shown. For the sake of clarity, individual data points are not presented since the curves are based on a total of 275 points. Data scatter was small, and approximately 90 percent of the data points are within ±0.02 of the $C_p/C_{p_{max}}$ values given by the faired curves. From the stagnation point to about 55 deg, there is no effect of Mach number on the distribution, which is lower than that predicted by the modified Newtonian theory. For values of θ greater than 55 deg, Mach number effects are apparent with the largest effect at the shoulder, θ = 90 deg. The variation of the shoulder pressure coefficient with Mach number is presented in Fig. 5. An empirical relation for this pressure coefficient as determined from Fig. 5b is

$$\left(\frac{C_p}{C_{p_{max}}}\right)_{\theta=90^\circ} = 0.0464 - \frac{0.511}{M_\infty^2} \tag{12}$$

For comparison, the results of two theoretical inviscid calculations and the result of a calculation (Van Dyke solution with method of characteristics) at M_∞ = 18 including a viscous boundary layer (Ref. 10) are included in Fig. 5. The inviscid solutions are consistently below the experimental data, and it may be seen that the effect of viscosity on the shoulder pressure is slight for the indicated conditions.

In Fig. 6, the stagnation point Mach number gradient, the sonic point location, and the pressure drag coefficient of the hemisphere are presented as functions of Mach number. For convenience, the stagnation point velocity gradient, $\beta D/u_\infty$, is also presented in Fig. 6. This curve was obtained by applying Eq. (2) to the faired data in Fig. 6a.

In determining θ^* from the M_∞ = 10 through 21 pressure data, a perfect gas flow with γ = 1.4 was assumed, i.e., gas imperfections were neglected. Included in the drag coefficients are force measurements by Nichols and Nierengarten (Ref. 13) which agree very well with the pressure measurements. Equations for $(dM/d\theta)_o$, θ^*, and C_D developed from the modified Newtonian theory indicate that these parameters are directly proportional to $1/M_\infty^2$. The data presented in Fig. 7 verify that this relation also applies to the experimental values of the parameters. Thus, empirical equations could be developed for each of the parameters:

$$\left(\frac{dM}{d\theta}\right)_o = 1.254 - \frac{0.510}{M_\infty^2}, \text{ 1/radian} \tag{13}$$

$$\theta^* = 41.44 + \frac{23.82}{M_\infty^2}, \text{ deg} \tag{14}$$

$$C_D = 0.901 - \frac{0.462}{M_\infty^2} \tag{15}$$

The data presented in Fig. 7, with the exception of the data from Ref. 12 which appeared to be consistently low, are within ±5 percent of the values given by these equations.

Also shown in Fig. 7 are the theoretical values predicted by the modified Newtonian theory and the Van Dyke-method of characteristics numerical solutions. The latter numerical values were obtained from the previously mentioned calculations of C. H. Lewis and from Ref. 26. There was some uncertainty (±2 percent) in the numerical solutions for θ^* and C_D as a result of inaccuracies in the computer computations.

Van Dyke (Ref. 27) suggested that the pressure distribution over the subsonic portion of a hemisphere could be represented by the power series,

$$\frac{p(\theta)}{p_{t_2}} = 1 - b_2\theta^2 - b_4\theta^4 - \cdots \tag{16}$$

If this relationship is substituted into Eq. (5), it is seen that the coefficient of θ^2 is given by

$$b_2 = \frac{\gamma}{2}\left(\frac{dM}{d\theta}\right)_o^2 \tag{17}$$

Thus, the value of this coefficient may be determined from Fig. 7a. For example, at an infinite Mach number the experimental data fairing gives $(dM/d\theta)_o$ = 1.254 and b_2 = 1.10, whereas Van Dyke's numerical solution gives b_2 = 1.20.

3.2 HEMISPHERE-CYLINDER

Surface pressure distributions on the hemisphere-cylinder, along the windward meridian line, at M_∞ = 10.05 and angles of attack from 0 to 25 deg are presented in Fig. 8. Data from both models are included and are in excellent agreement. Shown in the figure are axisymmetric (α = 0) numerical calculations for spherically blunted cones with half angles equal to the cylinder angle of attack. These results were obtained by C. H. Lewis using the Van Dyke solution matched to a method of characteristics solution (Ref. 24). Also shown are the theoretical values for sharp cones (Ref. 28). The theoretical results for the blunted cones predict the trends of the hemisphere-cylinder data very well, showing the expansion downstream of the shoulder and the subsequent compression to an asymptotic value. However, as would be expected, the cone solution does not accurately predict the pressure level on the hemisphere-cylinder because, except for α = 0, there are cross-flow effects on the cylinder which reduce the pressure below that predicted for an axisymmetric cone.

SECTION IV
CONCLUDING REMARKS

Surface pressure distributions were measured on a hemisphere-cylinder at a Mach number of 10.05 and at angles of attack up to 25 deg. These pressure distributions were compared with theoretical calculations and experimental results from tests at supersonic and hypersonic Mach numbers. The following results were obtained:

1. The M_∞ = 10.05 experimental pressure distribution on the hemisphere agrees very well with a numerical solution (Van Dyke-method of characteristics) from the stagnation point to about θ = 60 deg. For values of θ greater than 60 deg the modified Newtonian theory combined with a Prandtl-Meyer expansion is in good agreement with the data.
2. The pressure distribution on a hemisphere is independent of free-stream Mach number (M_∞ = 1.9 to 21) for $\theta < 55$ deg when presented as $C_p/C_{p_{max}}$. An empirical equation for the shoulder (θ = 90 deg) pressure was derived from the experimental data.
3. The modified Newtonian theory predicts the drag coefficient of spherical segments within four percent at M_∞ = 10.

4. Empirical relations for $(dM/d\theta)_o$, θ^*, and C_D as linear functions of $1/M_\infty^2$ were developed from experimental data for the Mach number range of 1.8 to 21. The Van Dyke numerical solution provides a better estimate of these characteristics than does the modified Newtonian theory. However, the modified Newtonian theory predicts these characteristics within five percent (except for C_D at $M_\infty < 2.2$) for the Mach number range investigated.

5. The pressures along the windward meridian line of the hemisphere-cylinder at angle of attack follow trends predicted by the axisymmetric numerical solution for a spherically blunted cone with half-angle equal to the cylinder angle of attack.

REFERENCES

1. Van Dyke, Milton D. "The Supersonic Blunt-Body Problem -- Review and Extension." Journal of the Aero/Space Sciences, Vol. 25, No. 8, August 1958, pp. 485-496.

2. Van Dyke, Milton D. and Gordon, Helen D. "Supersonic Flow Past a Family of Blunt Axisymmetric Bodies." NASA Technical Report R-1, 1959.

3. Lees, Lester. "Hypersonic Flow." Proc. 5th International Aeronautical Conference, Los Angeles, Institute of the Aeronautical Sciences, June 20-24, 1955.

4. Lees, Lester and Kubota, Toshi. "Inviscid Hypersonic Flow over Blunt-Nosed Slender Bodies." Journal of the Aeronautical Sciences, Vol. 24, No. 3, March 1957, pp. 195-202.

5. Baer, A. L. "Pressure Distributions on a Hemisphere Cylinder at Supersonic and Hypersonic Mach Numbers." AEDC-TN-61-96 (AD261501), August 1961.

6. Beckwith, Ivan E. and Gallagher, James J. "Heat-Transfer and Recovery Temperatures on a Sphere with Laminar, Transitional, and Turbulent Boundary Layers at Mach Numbers of 2.00 and 4.15." NACA TN 4125, December 1957.

7. Chauvin, Leo T. "Pressure Distribution and Pressure Drag for a Hemispherical Nose at Mach Numbers 2.05, 2.54, and 3.04." NACA RM L52K06, December 1952.

8. Cooper, Morton and Mayo, Edward E. "Measurements of Local Heat Transfer and Pressure on Six 2-Inch-Diameter Blunt Bodies at a Mach Number of 4.95 and at Reynolds Numbers Per Foot up to 81 x 10^6. NASA MEMO 1-3-59L, March 1959.

9. Crawford, Davis H. and McCauley, William D. "Investigation of the Laminar Aerodynamic Heat-Transfer Characteristics of a Hemisphere-Cylinder in the Langley 11-Inch Hypersonic Tunnel at a Mach Number of 6.8." NACA Report 1323, 1957.

10. Eaves, R. H. and Lewis, C. H. "Combined Effects of Viscous Interaction and Ideal Source Flow on Pressure and Heat-Transfer Distribution over Hemisphere Cylinders at Mach 18." AEDC-TR-65-158 (AD467447), July 1965.

11. Kendall, James M., Jr. "Experiments on Supersonic Blunt-Body Flows." Jet Propulsion Laboratory Progress Report No. 20-372, February 1959.

12. Korobkin, Irving. "Laminar Heat Transfer Characteristics of a Hemisphere for the Mach Number Range 1.9 to 4.9." NAVORD Report 3841, October 1954.

13. Nichols, James O. and Nierengarten, Edward A. "Aerodynamic Characteristics of Blunt Bodies." Jet Propulsion Laboratory Technical Report No. 32-677, November 1964.

14. Oliver, Robert E. "An Experimental Investigation of Flow over Simple Blunt Bodies at a Nominal Mach Number of 5.8." GALCIT Memorandum No. 26, June 1955.

15. Perkins, Edward W., Jorgensen, Leland H., and Sommer, Simon C. "Investigation of the Drag of Various Axially Symmetric Nose Shapes of Fineness Ratio 3 for Mach Numbers from 1.24 to 7.4." NACA Report 1386, 1958.

16. Reichle, Henry G., Jr. "Hemisphere-Cylinder Pressure Distributions at Subsonic, Transonic, and Supersonic Mach Numbers." George C. Marshall Space Flight Center, MTP-AERO-62-30, March 1962.

17. Stalder, Jackson R. and Nielsen, Helmer V. "Heat Transfer from a Hemisphere-Cylinder with Flow-Separation Spikes." NACA TN 3287, September 1954.

18. Stine, Howard A. and Wanlass, Kent. "Theoretical and Experimental Investigation of Aerodynamic-Heating and Isothermal Heat-Transfer Parameters on a Hemispherical Nose with Laminar Boundary Layer at Supersonic Mach Numbers." NACA TN 3344, December 1954.

19. Winkler, E. M. and Danberg, J. E. "Heat-Transfer Characteristics of a Hemisphere Cylinder at Hypersonic Mach Numbers." NAVORD Report 4259, April 1957.

20. Zakkay, Victor. "An Investigation of the Location of the Sonic Point on Various Spherically Blunted Bodies." GASL Technical Report No. 114, July 1959.

21. AGARD Wind Tunnel and Model Testing Panel. "AGARD Wind Tunnel Calibration Models." AGARD Specification 2, September 1957.

22. Lukasiewicz, J. "Hypersonic Flow-Blast Analogy." AEDC-TR-61-4 (AD259455), June 1961; ARS Journal, Vol. 32, No. 9, September 1962, pp. 1341-1346.

23. Test Facilities Handbook (Fifth Edition). von Kármán Gas Dynamics Facility, Vol. 4." Arnold Engineering Development Center, July 1963.

24. Roberts, J. F., Lewis, Clark H., and Reed, Marvin. "Ideal Gas Spherically Blunted Cone Flow Field Solutions at Hypersonic Conditions." AEDC-TR-66-121 (AD637703), August 1966.

25. Fay, J. A. and Riddell, F. R. "Theory of Stagnation Point Heat Transfer in Dissociated Air." Journal of the Aeronautical Sciences, Vol. 25, No. 2, February 1958, pp. 73-85.

26. Sims, J. L. "Results of Calculations of Supersonic Flow Fields about Spherical Capped Bodies of Revolution." George C. Marshall Space Flight Center, MTP-AERO-62-40, May 1962.

27. Van Dyke, Milton. "Second-Order Compressible Boundary-Layer Theory with Application to Blunt Bodies in Hypersonic Flow." AFOSR-TN-61-1270, July 1960.

28. Anon. "Equations, Tables, and Charts for Compressible Flow." NACA Report 1135, 1953.

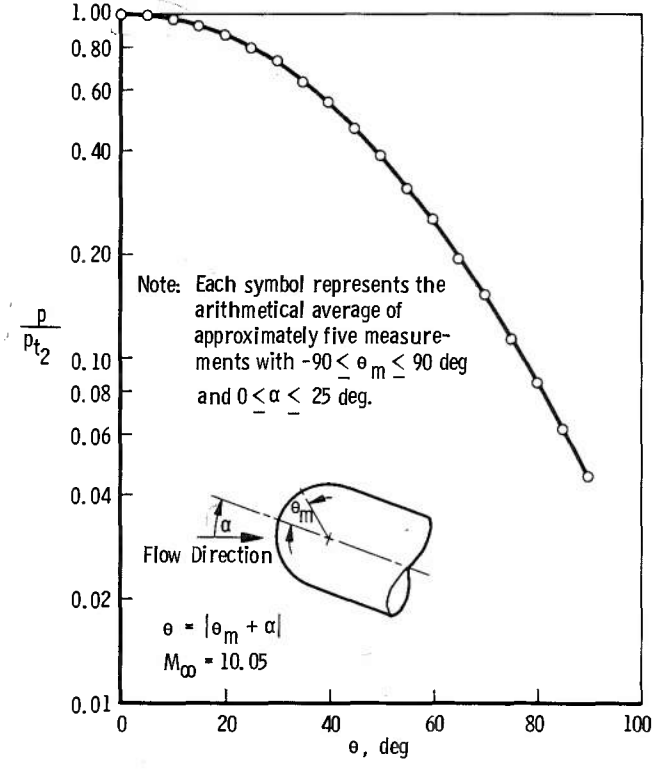

a. Experimental Distribution

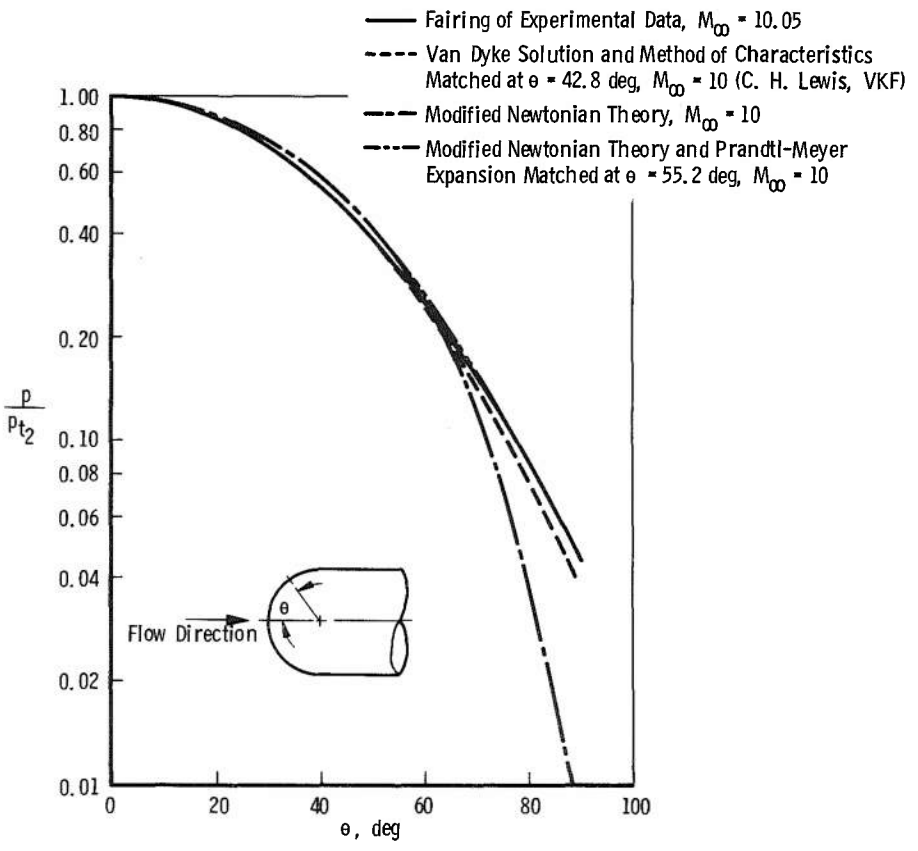

b. Comparison of Experimental and Theoretical Distributions

Fig. 1 Hemisphere Pressure Distribution, M_∞ = 10

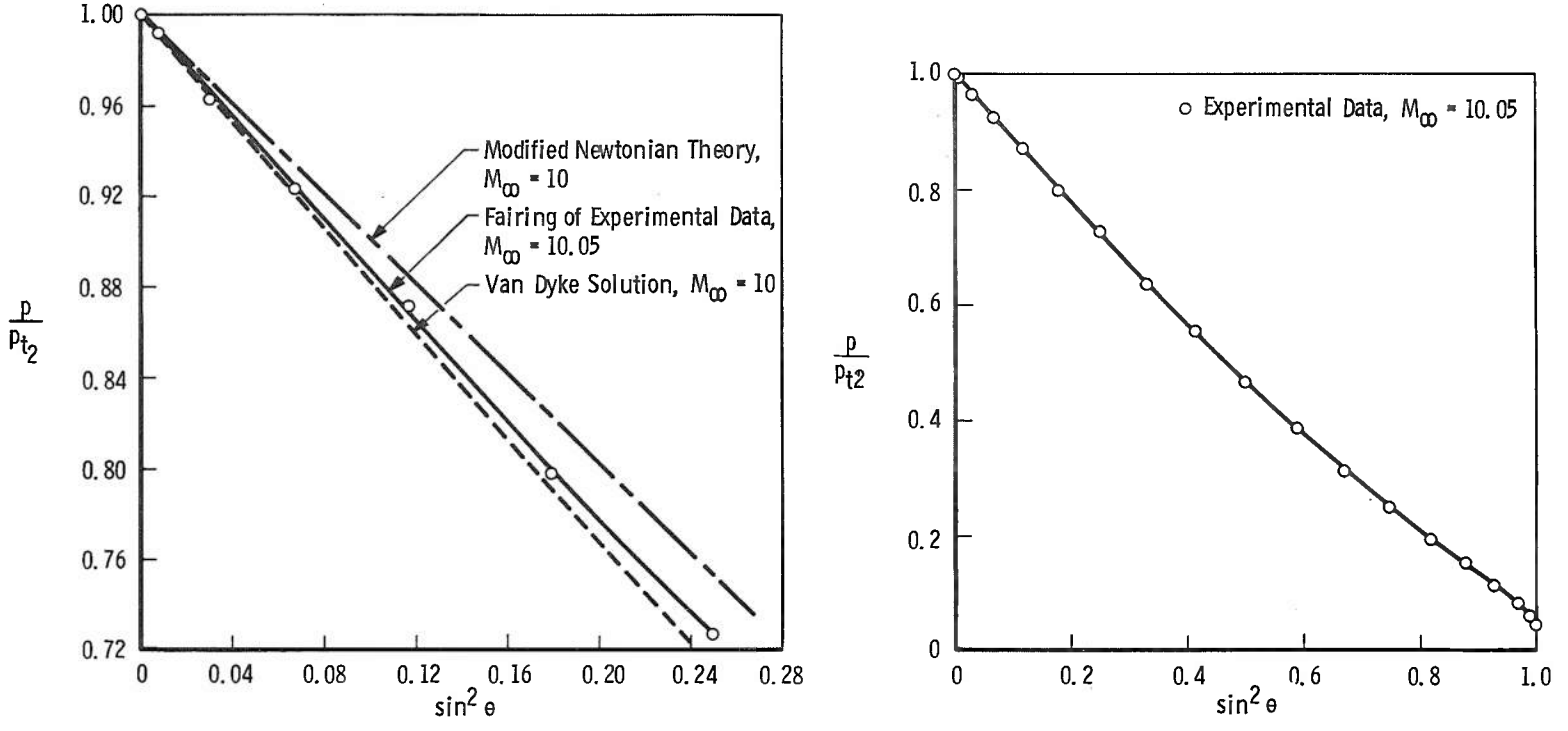

Fig. 2 Variation of p/p_{t_2} with $\sin^2\theta$, $M_\infty = 10$

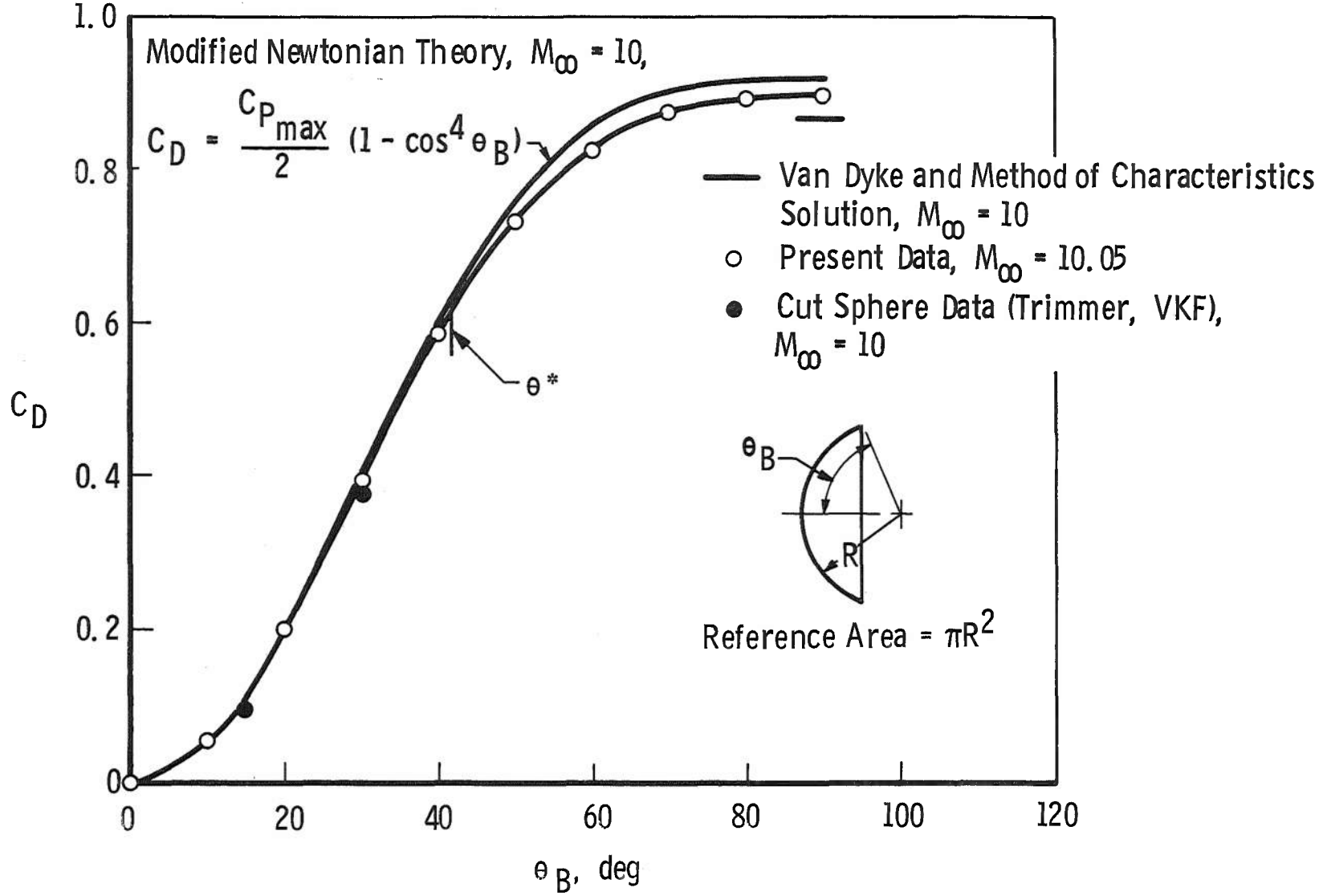

Fig. 3 Variation of Drag Coefficient with θ_B for Spherical Segments, M_∞ = 10

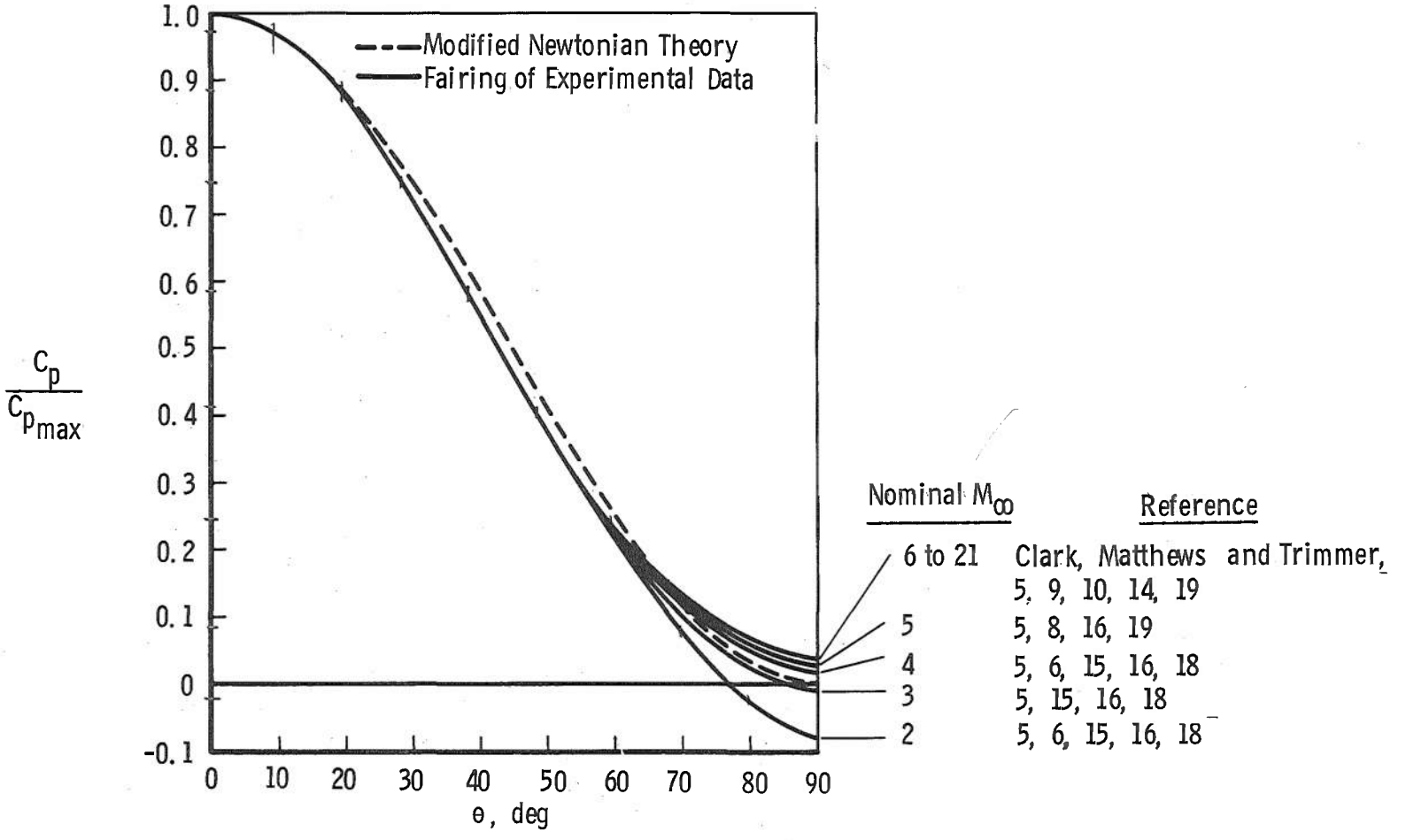

Fig. 4 Hemisphere Pressure Distribution, M_∞ = 1.9 to 21

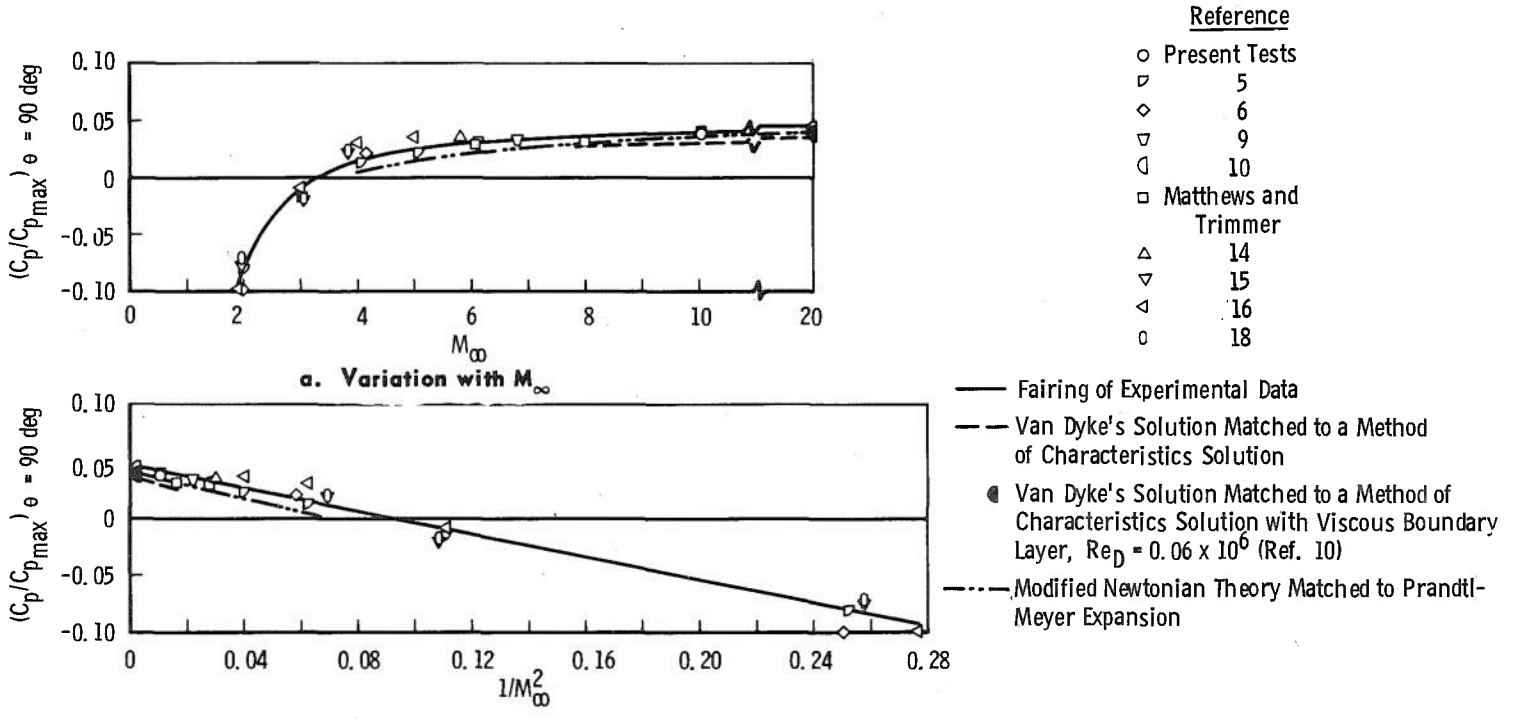

Fig. 5 Variation of Hemisphere Shoulder (θ = 90 deg) Pressure with Mach Number

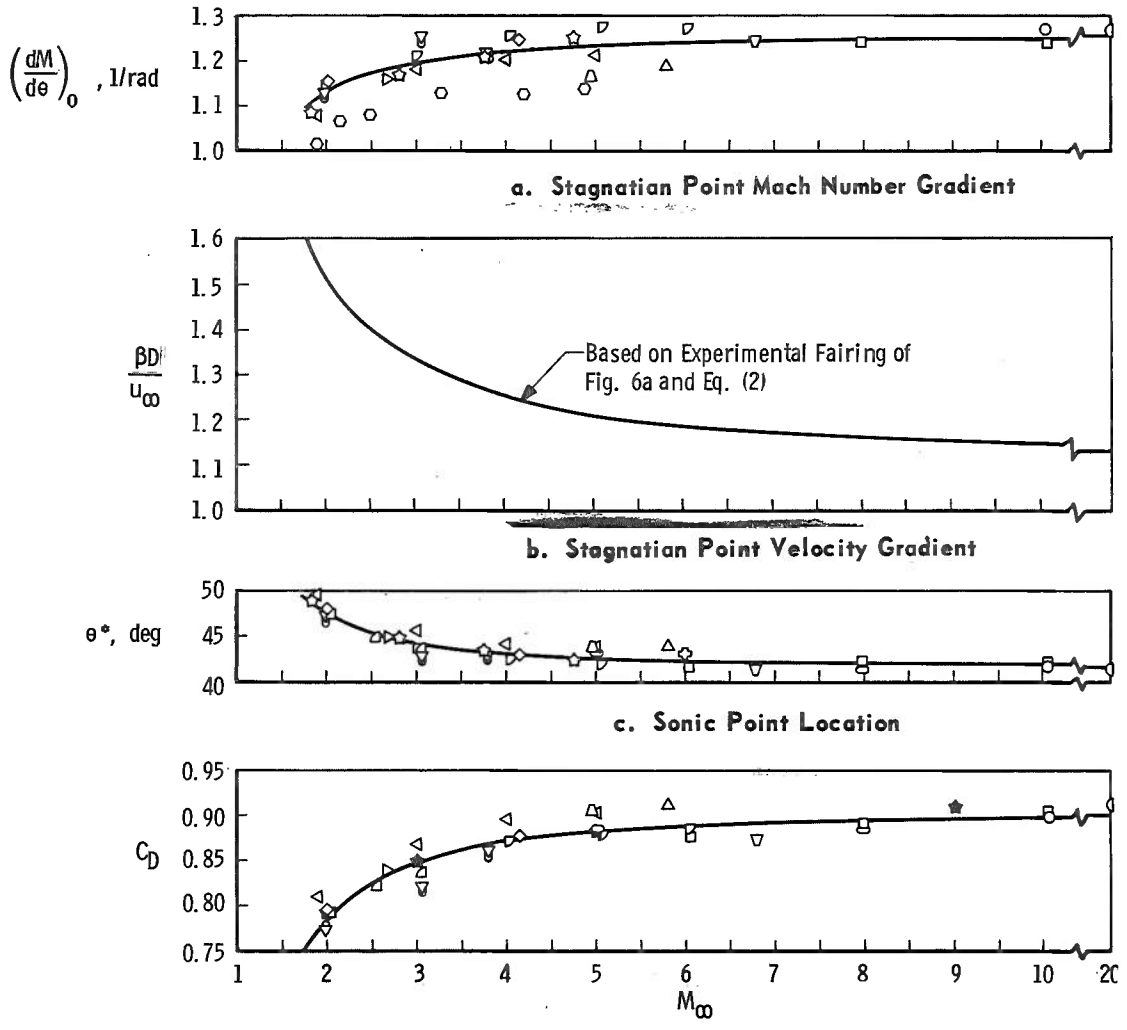

Reference	
○	Present Tests
▷	5
◇	6
◁	7
△	8
▽	9
◁	10
☆	11
○	12
□	Matthews & Trimmer
△	14
▽	15
◁	16
▷	17
○	18
○	19
☆	20
★	13 (Force Data)

Fig. 6 Variation of Hemisphere Characteristics with M_∞

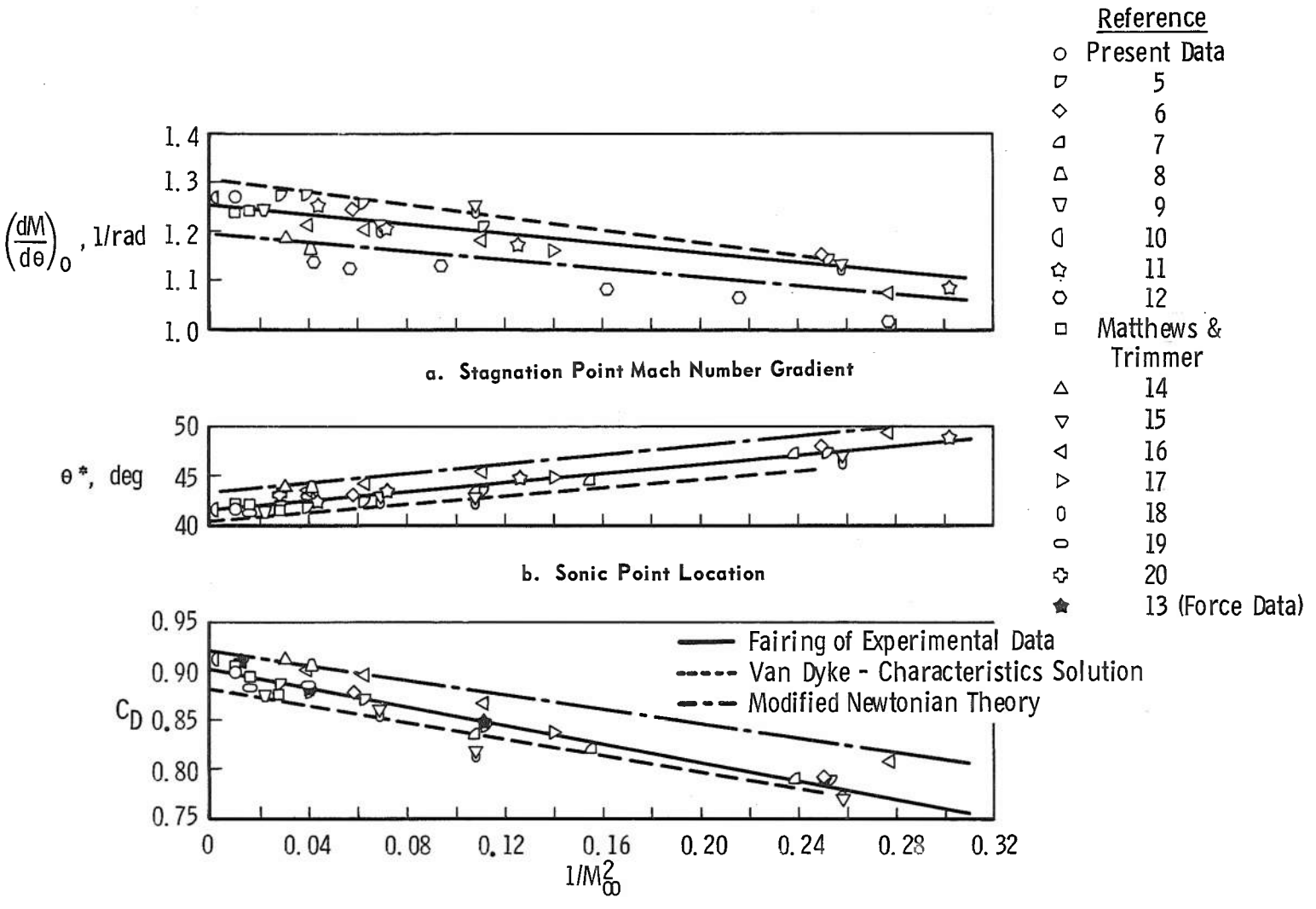

a. Stagnation Point Mach Number Gradient

b. Sonic Point Location

c. Drag Coefficient

Fig. 7 Variation of Hemisphere Characteristics with $1/M_\infty^2$

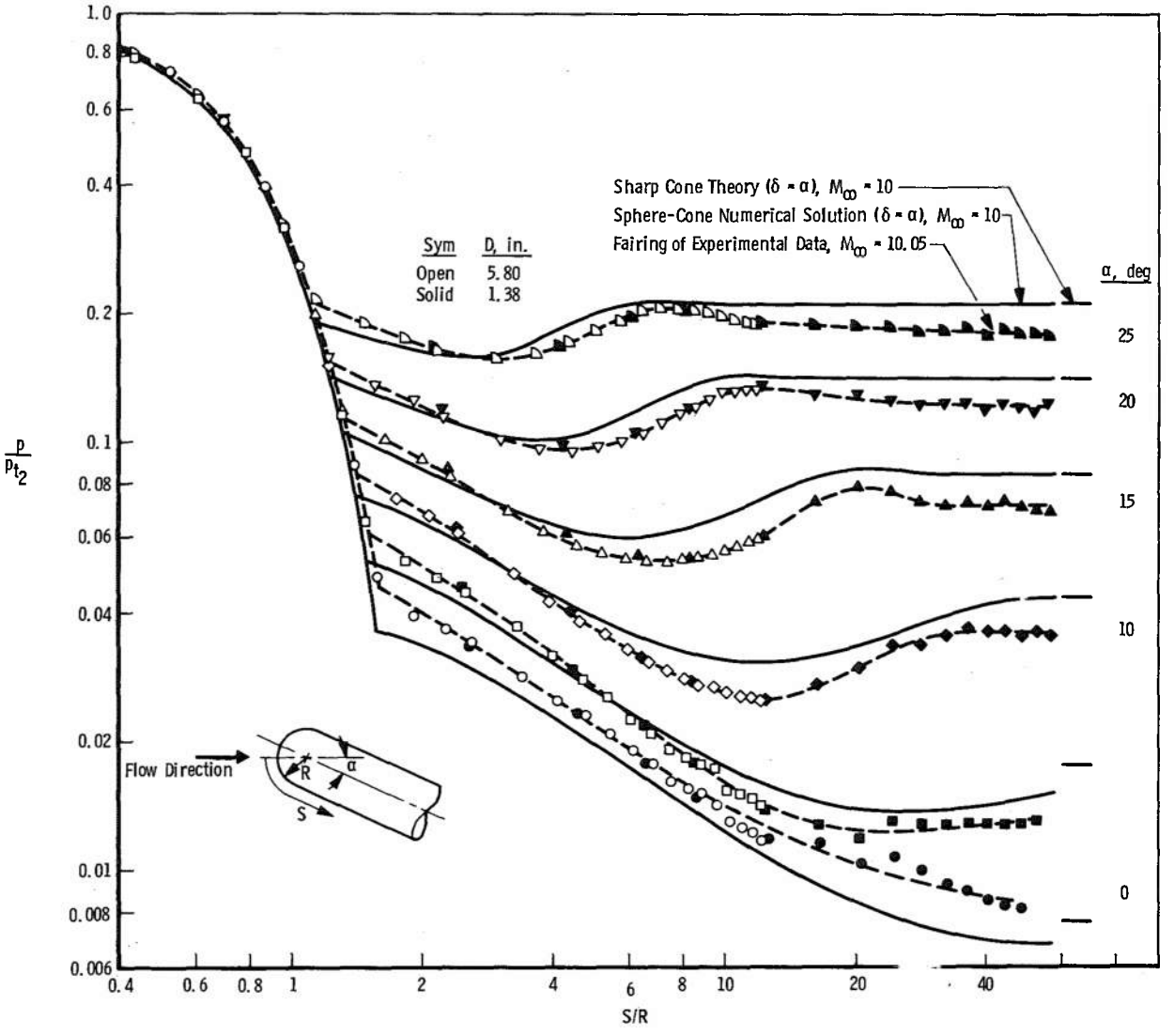

Fig. 8 Hemisphere-Cylinder Pressure Distribution along the Windward Meridian Line, M_∞ = 10

TABLE I
EXPERIMENTAL PRESSURE RATIOS FOR HEMISPHERE, $M_\infty = 10.05$, $R_{e_D} = 0.63 \times 10^6$

θ, deg	p/p_{t_2}	θ, deg	p/p_{t_2}
0	1.000	50	0.388
5	0.992	55	0.312
10	0.963	60	0.252
15	0.923	65	0.194
20	0.871	70	0.152
25	0.798	75	0.114
30	0.727	80	0.085
35	0.637	85	0.062
40	0.555	90	0.046
45	0.467		

Note: These tabulated pressure ratios are the arithmetical averages of four to six measurements at each value of θ.

TABLE II
SUMMARY OF TEST CONDITIONS FOR REFERENCED DATA

Source	Reference	M_∞	D, in.	$Re_D \times 10^{-6}$
Present Tests (AEDC-VKF)	---	10.05	5.80	0.6
Baer (AEDC-VKF)	5	1.99	5.80	1.0
		3.00	↓	2.0
		4.03	↓	2.6
		5.06	↓	3.0
		6.03	↓	2.2
Beckwith & Gallagher (NACA-LAL)	6	2.00	3.5	4.6-9.6
		4.15	↓	6.7-9.1
Chauvin (NACA-LAL)	7	2.05	3.98	4.4
		2.54	↓	4.6
		3.04	↓	4.2
Cooper & Mayo (NASA-LRC)	8	4.95	2.0	8-13
Crawford & McCauley (NACA-LAL)	9	6.8	3.0	0.5-1.0
Eaves & Lewis (AEDC-VKF)*	10	18-21	4.0	0.02-0.10
Kendall (JPL-CIT)	11	1.82	3.0	
		2.81	↓	
		3.74	↓	
		4.76	↓	
Korobkin (NOL)	12	1.90	2.0	0.7
		2.15	↓	0.6
		2.48	↓	0.5
		3.26	↓	0.4
		4.20	↓	0.2
		4.87	↓	0.2
Matthews & Trimmer (AEDC-VKF)	--	6.04	5.8	1.3
		7.98	↓	0.9
		10.08	↓	0.6
Nichols & Nierengarten (JPL-CIT)**	13	2.01	3.0	1.0
		3.02	↓	1.0
		5.01	↓	0.4
		9.02	↓	0.3

*Data obtained at a wall to free-stream stagnation temperature ratio of 0.062 to 0.12, whereas data from other references were obtained at or near equilibrium conditions.

**Force data

TABLE II (Concluded)

Source	Reference	M_∞	D, in.	$Re_D \times 10^{-6}$
Oliver (GALCIT)	14	5.8	1.0	0.2
Perkins, Jorgensen & Sommer (NACA-AAL)	15	1.97	4.0	4.0
		3.04	↓	4.0
		3.80	↓	4.0
Reichle (NASA-MSFC)	16	1.9	1.50	1.0
		3.0	↓	0.7
		4.0	↓	0.4
		5.0	↓	0.4
Stalder & Nielsen (NACA-AAL)	17	2.67	1.0	0.2-0.7
Stine & Wanlass (NACA-AAL)	18	1.97	4.0	3.0-6.6
		3.04	↓	2.8-4.0
		3.80	↓	2.8
Winkler & Danberg (NOL)	19	5.01	1.5	0.1-0.8
		7.97	↓	0.1-0.3
Zakkay (GASL)	20	6.0	1.0	0.3

DOCUMENT CONTROL DATA - R&D

(Security classification of title, body of abstract and indexing annotation must be entered when the overall report is classified)

1. ORIGINATING ACTIVITY *(Corporate author)* Arnold Engineering Development Center ARO, Inc., Operating Contractor Arnold Air Force Station, Tennessee	2a. REPORT SECURITY CLASSIFICATION UNCLASSIFIED 2b. GROUP N/A

3. REPORT TITLE

HEMISPHERE-CYLINDER PRESSURE DISTRIBUTIONS AT SUPERSONIC AND HYPERSONIC MACH NUMBERS

4. DESCRIPTIVE NOTES *(Type of report and inclusive dates)*

N/A

5. AUTHOR(S) *(Last name, first name, initial)*

Clark, E. L., ARO, Inc.

6. REPORT DATE	7a. TOTAL NO. OF PAGES	7b. NO. OF REFS
December 1966	30	28

8a. CONTRACT OR GRANT NO. AF 40(600)-1200 b. Program Element 65402234 c. d.	9a. ORIGINATOR'S REPORT NUMBER(S) AEDC-TR-66-179 9b. OTHER REPORT NO(S) *(Any other numbers that may be assigned this report)* N/A

10. AVAILABILITY/LIMITATION NOTICES This document is subject to special export controls and each transmittal to foreign governments or foreign nationals may be made only with prior approval of the Arnold *

11. SUPPLEMENTARY NOTES Available in DDC.	12. SPONSORING MILITARY ACTIVITY Arnold Engineering Development Center Air Force Systems Command Arnold Air Force Station, Tennessee

13. ABSTRACT

Pressure distributions on a hemisphere-cylinder at a Mach number of 10 and at angles of attack up to 25 deg are presented. These experimental distributions are compared with hypersonic blunt-body analytical and numerical solutions. Experimental stagnation point velocity gradients, sonic point locations, and pressure drag coefficients for hemispheres at Mach numbers from 1.8 to 21 have been compiled, and empirical relations are developed for these parameters as functions of Mach number.

* Engineering Development Center (AETS).

DD FORM 1 JAN 64 1473

14. KEY WORDS	LINK A		LINK B		LINK C	
	ROLE	WT	ROLE	WT	ROLE	WT
pressure testing aerodynamic forces hemisphere-cylinders blunt bodies pressure drag supersonic flow hypersonic flow						

INSTRUCTIONS

1. ORIGINATING ACTIVITY: Enter the name and address of the contractor, subcontractor, grantee, Department of Defense activity or other organization *(corporate author)* issuing the report.

2a. REPORT SECURITY CLASSIFICATION: Enter the overall security classification of the report. Indicate whether "Restricted Data" is included. Marking is to be in accordance with appropriate security regulations.

2b. GROUP: Automatic downgrading is specified in DoD Directive 5200.10 and Armed Forces Industrial Manual. Enter the group number. Also, when applicable, show that optional markings have been used for Group 3 and Group 4 as authorized.

3. REPORT TITLE: Enter the complete report title in all capital letters. Titles in all cases should be unclassified. If a meaningful title cannot be selected without classification, show title classification in all capitals in parenthesis immediately following the title.

4. DESCRIPTIVE NOTES: If appropriate, enter the type of report, e.g., interim, progress, summary, annual, or final. Give the inclusive dates when a specific reporting period is covered.

5. AUTHOR(S): Enter the name(s) of author(s) as shown on or in the report. Enter last name, first name, middle initial. If military, show rank and branch of service. The name of the principal author is an absolute minimum requirement.

6. REPORT DATE: Enter the date of the report as day, month, year, or month, year. If more than one date appears on the report, use date of publication.

7a. TOTAL NUMBER OF PAGES: The total page count should follow normal pagination procedures, i.e., enter the number of pages containing information.

7b. NUMBER OF REFERENCES: Enter the total number of references cited in the report.

8a. CONTRACT OR GRANT NUMBER: If appropriate, enter the applicable number of the contract or grant under which the report was written.

8b, 8c, & 8d. PROJECT NUMBER: Enter the appropriate military department identification, such as project number, subproject number, system numbers, task number, etc.

9a. ORIGINATOR'S REPORT NUMBER(S): Enter the official report number by which the document will be identified and controlled by the originating activity. This number must be unique to this report.

9b. OTHER REPORT NUMBER(S): If the report has been assigned any other report numbers *(either by the originator or by the sponsor)*, also enter this number(s).

10. AVAILABILITY/LIMITATION NOTICES: Enter any limitations on further dissemination of the report, other than those imposed by security classification, using standard statements such as:

(1) "Qualified requesters may obtain copies of this report from DDC."

(2) "Foreign announcement and dissemination of this report by DDC is not authorized."

(3) "U. S. Government agencies may obtain copies of this report directly from DDC. Other qualified DDC users shall request through _____."

(4) "U. S. military agencies may obtain copies of this report directly from DDC. Other qualified users shall request through _____."

(5) "All distribution of this report is controlled. Qualified DDC users shall request through _____."

If the report has been furnished to the Office of Technical Services, Department of Commerce, for sale to the public, indicate this fact and enter the price, if known.

11. SUPPLEMENTARY NOTES: Use for additional explanatory notes.

12. SPONSORING MILITARY ACTIVITY: Enter the name of the departmental project office or laboratory sponsoring *(paying for)* the research and development. Include address.

13. ABSTRACT: Enter an abstract giving a brief and factual summary of the document indicative of the report, even though it may also appear elsewhere in the body of the technical report. If additional space is required, a continuation sheet shall be attached.

It is highly desirable that the abstract of classified reports be unclassified. Each paragraph of the abstract shall end with an indication of the military security classification of the information in the paragraph, represented as *(TS), (S), (C), or (U)*.

There is no limitation on the length of the abstract. However, the suggested length is from 150 to 225 words.

14. KEY WORDS: Key words are technically meaningful terms or short phrases that characterize a report and may be used as index entries for cataloging the report. Key words must be selected so that no security classification is required. Identifiers, such as equipment model designation, trade name, military project code name, geographic location, may be used as key words but will be followed by an indication of technical context. The assignment of links, rules, and weights is optional.